Chapter -4

PARAMETER ESTIMATION AND COMPUTATIONAL PROCEDURES

4.0 General

In the mathematical modeling (given in Chapter 3), the number of required or estimated parameters, depends on the type of problems. Description of the problem in present chapter identifies following parameters to be either known or estimated: (i) CMOD rate functions and (ii) crack parameters (number, locations and geometry of cracks). These estimated or known parameters then close the equations of mathematical modeling presented in Chapter 3. CMOD rate functions under the influence of creep in FPZ have been proposed based on the literature review presented in Chapter 2. As discussed in Chapter 2, the determination of crack parameters is very difficult. Therefore, the crack parameters at upstream face of the dam have been arrived by trial and error procedure. Those crack parameters, which give the convergent solution of dam-crown deflections, presented in Chapter 5, has been described in present chapter.

After estimating these parameters, inter related computational procedures for the solution of transient uplift pressure, dam-crown deflections and factor of safety in sliding are discussed.

4.1 Problem Description

Rihand Dam a concrete gravity dam of 3065 ft. (934.21m.) length is situated in Sonebhadra district of Uttar Pradesh, India. It is 91.44m high and traps river Rihand which is a tributary of river Sone. The dam comprises of 61 blocks of width ranging from 12.80m to 18.30 m with un-grouted joints. Block no. 1 - 27 and 48 - 60 are non-overflow blocks. Block no. 28 - 33 constitute intake and Power House unit, while the spillway is situated on block no. 34 – 47. The Power House was commissioned in the year 1962 with 5 units of 50 MW each, and the sixth unit of 50 MW was added in 1966.

It is purely a Hydro - Power generation project with reservoir capacity of 8.6 million Acre ft. at F.R.L. 268.22 m (880.00 ft.). The Power House is situated at the toe of the dam with generating capacity of 300 M.W. The original dead storage level of the reservoir was 232.22m (775 ft.) with live storage of 7.28 million acre ft. In due course of time several thermal power projects were established on the periphery of the reservoir. For providing cooling water to these thermal power projects, the dead storage level was raised to 252.98 m (830 ft) in 1984 and the live storage capacity has now reduced to 4.65 million acre ft. A typical non-overflow cross section of the dam is prepared and given in the Fig.4.1.

Within few years of commissioning of project in 1962, cracks began to appear in the various components of the dam and appurtenant works. Distresses have since been observed in the dam and related structures. After the detailed study, the members of the expert committee (Chief Engineer (Sone), 2011a, b) have given the opinion that the cracks in the body of the dam were developed due to either or a combination of the following.

- Expansion of concrete due to alkali-aggregate reaction.
- Effect of temperature variation.

- Possible deformability of foundation rock especially in the vicinity of the downstream toe of the dam.

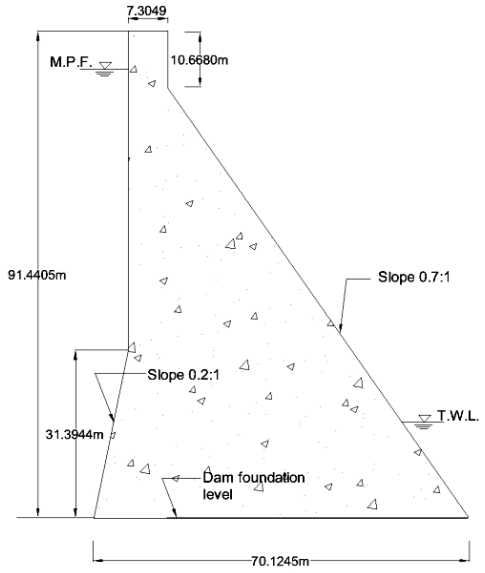

Fig.4.1. A typical cross-section of Rihand dam at non-overflow location.

Later studies also revealed qualitatively that creep phenomenon are effective in controlling the dam-crown deflection. But its effect combined with the crack in dam has not been studied quantitatively.

Therefore, the present work is an effort to provide a model to compute dam-crown deflection by incorporating indirectly the effect of FPZ based creep effect on CMOD-rate under monthly reservoir variation.

4.1.1 Data Availability and Assumptions

To validate the proposed model, sufficient data is needed. But in present case, only monthly reservoir level versus dam-crown deflection data for six years

(2005-06 to 2010-11) are available as per the record (Chief Engineer (Sone), 2011 b). Following essential data are unfortunately not available.

- CMOD and its rate.
- Location and length of cracks located at upstream face of the dam
- Crack geometry i.e. width, roughness etc.
- Extent of creep in fracture process zone (FPZ)

Therefore a number of assumptions regarding the above set of unavailable data are made and tested in proposed dam-crown deflection model. In subsequent discussions the assumptions of these data correspond to the convergent result of proposed dam-crown deflection model presented in Chapter 5.

4.2 Crack Mouth Opening Displacement (CMOD) Rate Formulation

For the calculation of transient pressure along the crack, CMOD and its rate are the specified variables. CMOD, as function of time and hence its rate are known either from seismic data or it can be generated in controlled laboratory experiment. However, under the cyclic loading and presence of influencing factors like creep, alkali-silica-reaction (ASR) and mutual interaction of multiple cracks in concrete dams, the determination of time variation of CMOD is very difficult. On basis of literature review (presented in Chapter 2), the CMOD as a function of time is presented and verified indirectly through its use in the determination of dam crown deflection discussed in Chapter 5.

To study the influence of CMOD-rate on the specific fracture energy and the strain softening diagram, under fast monotonic loading rate, Bruhwiler and Wittmann (1990) proposed the following CMOD-rate relation on the basis of the wedge-splitting (WS) tests results.

$$b_m = c(\dot{b}_m)^{n_0} \tag{4.1}$$

Where $c$and n_0 are constants. In the present study, time variation of CMOD before peak loading is modeled by sine function, while post-peak CMOD is represented by equation (4.1), under following set of assumptions.

- In addition to creep phenomenon occurring in FPZ, interaction of multiple cracks and fatigue are accounted for in these equations.
- Exponent n_0 is taken as unity (Table 4.1).Thus equation (4.1) is written as

$$b_m = -c\dot{b}_m \tag{4.2}$$

- Loading is sudden and occur at the beginning of time interval chosen.
- Pre-peak CMOD-time variation corresponds to crack-opening while post-peak CMOD-time relation represents the crack-closing phase.
- During loading which correspond to opening mode, the crack tip stress is less than or equal to material strength at maximum loading and creep in FPZ is effectively contributing to CMOD.
- During unloading which correspond to closing mode, effect of non-linear creep in FPZ follows the equation (4.2).
- CMOD and its rate are generated over one cycle of opening and closing phase which correspond to one opening-closing cycle of the given problem on reduced time scale.

On the basis of above assumptions, CMOD-time relations for opening and closing mode can be written as follows.

Opening Mode

For opening mode, CMOD generating function is assumed as

$$b_m = a_0 + b_0 \sin\left(\omega t + \theta\right) \tag{4.3}$$

Where $\omega = 2\pi/T$, θ is phase angle and T is the time period of one opening-closing cycle. This function is generated only for half cycle representing only opening mode. The constant a_0 is introduced to take into account the residual opening. In mathematical modeling, parameters of this equation are calculated using given or assumed boundary conditions.

Closing Mode

After integration equation (4.2), the resulting equation can be written as

$$b_m = b_c e^{-kt} \tag{4.4}$$

Where b_c and k are constants and can be determined using boundary conditions in the mathematical modeling.

Boundary Conditions

It is assumed that

- Crack starts to open and close at residual CMOD,b_{mr} and reaches to maximum value of CMOD,b_{max}at time $T/2$.
- CMOD- rate at beginning and at $T/2$is zero.

Symbolically above statements can be written as

$$b_m = \begin{cases} b_{mr} & When \quad t = 0 \\ b_{\max} & \quad\quad\;\; t = T/2 \\ b_{mr} & \quad\quad\;\; t = T \end{cases} \tag{4.5}$$

and

$$\dot{b}_m = 0 \quad (when \quad t = 0 \quad and \quad T/2) \tag{4.6}$$

Using the above boundary conditions, equations (4.3) and (4.4) are simplified and written as

$$b_m = \begin{cases} \left(\frac{b_{\max}+b_{mr}}{2}\right)+\left(\frac{b_{\max}-b_{mr}}{2}\right)\sin\left(\omega t+\frac{3\pi}{4}\right) & (opening \quad mode) \\ \left(\frac{b_{\max}^2}{b_{mr}}\right)\exp\left\{-\frac{2}{T}\ln\left(\frac{b_{\max}}{b_{mr}}\right)t\right\} & (closing \quad mode) \end{cases} \tag{4.7}$$

Maximum and minimum (residual) values of CMOD, value of exponent n_0 in exponential CMOD generating function and opening-closing time-period, chosen on the trial and error basis, and adopted for convergent solution of dam-crown deflections, are shown in the Table 4.1.

Table 4.1. Trial and adopted crack parameters in present model.

Crack Parameters	Unit	Trial values	Adopted values
Maximum CMOD (b_{max})	mm	2.5, 2.0, 1.5	1.5
Residual CMOD (b_{mr})	mm	1.0,0.5,0.5	0.5
Exponent n_0	-	0.05,0.5,0.75,1.0	1.0
Time period	second	12,6	6

Adopted time period is divided into 12 time-intervals of 0.5 second each with the assumption that these time intervals, used in the CMOD generating function, represent the one month time interval in prototype. It is assumed that sustained hydrostatic load, due to change of monthly reservoir level , is applied at the beginning of the monthly time- interval, over which creep effect in FPZ is causing crack mouth to change.

Using the above crack parameters, sinusoidal and exponential CMOD generating functions can be written as

$$b_m = \begin{cases} 1.0 + 0.5\sin\left(\frac{t}{3} + \frac{3}{4}\right)\pi \quad mm \quad (opening \quad mode) \\ 4.5e^{-0.366t} \quad mm \quad (closing \quad mode) \end{cases} \tag{4.8}$$

Above equation is represented graphically in Figure 4.2 with horizontal axis representing the monthly time.

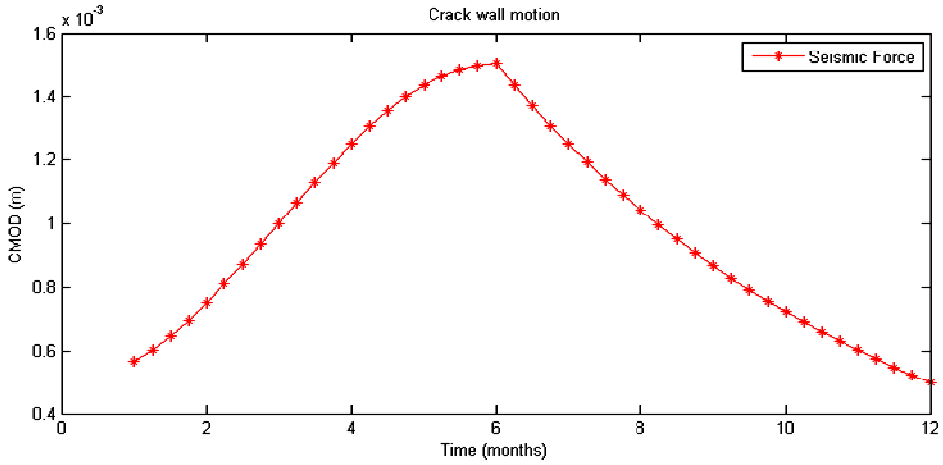

Fig.4.2. CMOD versus time (month) under FPZ creep effect.

4.3 Crack lengths and Locations

Horizontal wedge-shaped cracks with unit width are assumed. Because of uncertain (i) fracture parameters, (ii) fatigue parameters and (iii) cracks interaction behavior, lengths and locations of effective cracks lying along the upstream face, between heel and slope changing point are assumed on trial and error basis and adopted for convergent solution of dam-crown deflection, presented in chapter 5. After numerous attempts, four effective cracks (Fig.4.3) are identified: (1) Crack-1 at EL 0.00 (Heel) (2) Crack-2 at EL 10.4648m (3) Crack-3 at EL 20.9296m (4) Crack-4 at EL 31.3944m (Slope-changing point).

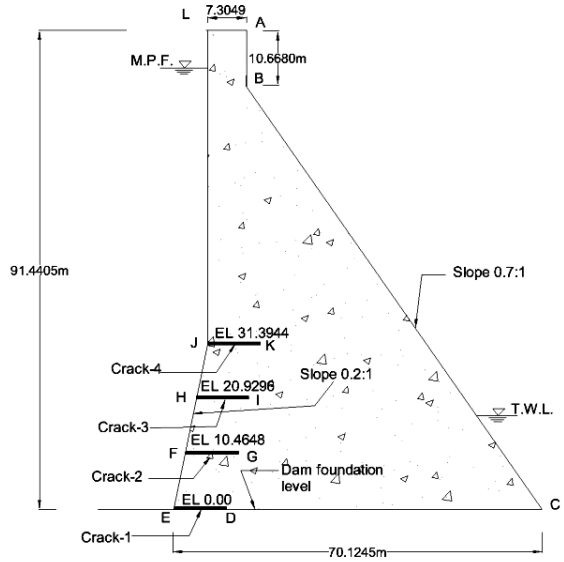

Fig.4.3. Locations of cracks in the body.

Changes in the lengths of these cracks are assumed on annual basis. These changes are assumed on trial and error basis, in the light of above mentioned reasons. Table 4.2 shows the adopted crack lengths for different year for convergent solution of dam-crown deflections.

Table 4.2. Length of Cracks in different years.

Crack Location	Adopted Length (m) (Year- wise)					
	2005-06	**2006-07**	**2007-08**	**2008-09**	**2009-10**	**2010-11**
Crack-1	10	10.25	10.45	10.56	10.62	10.71
Crack-2	10	10.20	10.40	10.48	10.54	10.63
Crack-3	10	10.15	10.28	10.39	10.44	10.52
Crack-4	10	10.10	10.22	10.32	10.38	10.43

4.4 Computational Procedures

Computational procedures essentially consist of three parts: (i) calculation of transient uplift pressure caused due to crack wall motion, (ii) dam-crown deflections under monthly reservoir level variations and (iii) stability analysis of dam in sliding. Fig.4.4 shows the overall flow chart for calculation of stability and deflection of a concrete gravity dam considering transient variation of uplift pressure in cracks. Assumed or estimated model parameters and material properties are provided as input data.

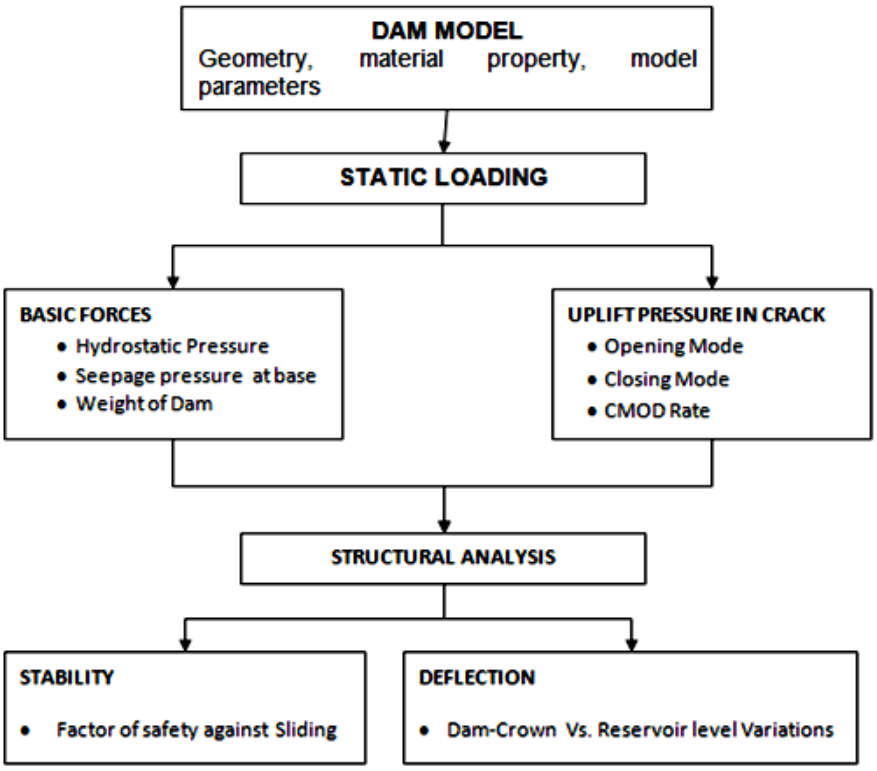

Fig. 4.4 Overall flow chart for dam model.

Transient uplift pressures in the cracks are calculated separately for opening and closing cycle of the crack wall motion. A general flow chart for calculating the transient uplift pressure is given in Figs. 4.5, 4.6 and 4.7.

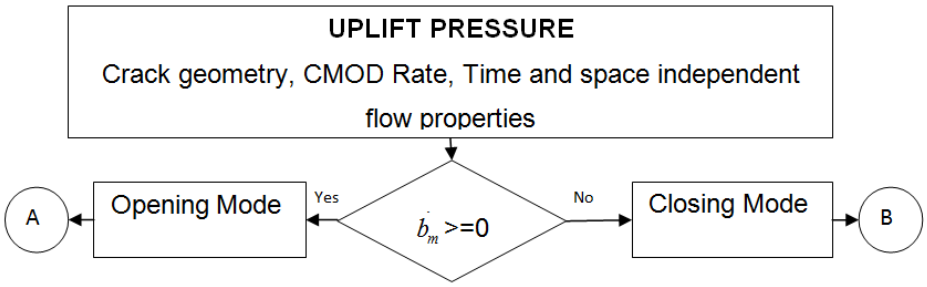

Fig.4.5. A composite flow chart of uplift pressure calculation for opening and closing mode of the crack.

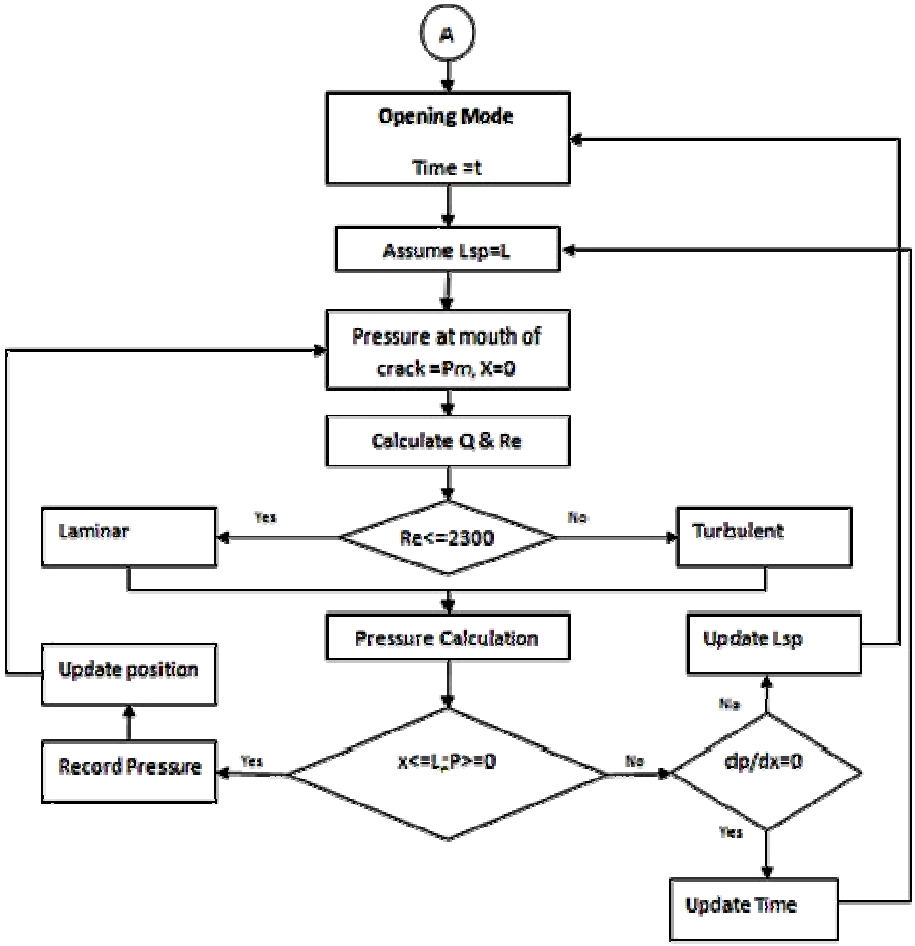

Fig.4.6. Flow chart for calculating the uplift pressure during opening mode of the crack.

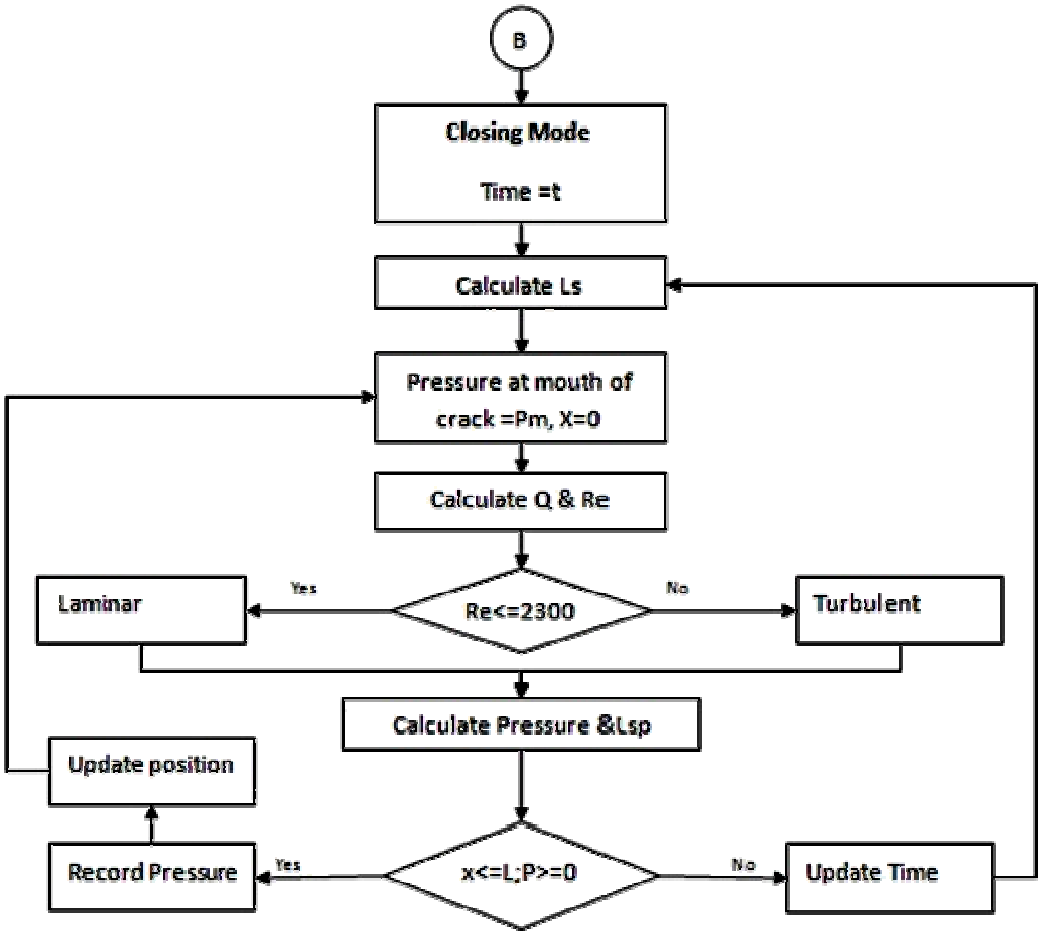

Fig.4.7. Flow chart for calculating the uplift pressure during closing mode of the crack.

Computed uplift pressures in different cracks at given monthly reservoir level are used with other imposed loads to calculate the dam-crown deflections. Reservoir level versus calculated dam-crown deflections are plotted and compared with field data. Assumed and estimated parameters discussed above, are changed iteratively or on trial and error basis and used after achieving desired accuracy in calculated dam-crown deflection. A flow chart for calculating the dam-crown deflection has been presented in Fig.4.8. Uplift pressure in cracks, calculated using MATLAB (version 2013) software, is

imported in the ANSYS (version 15.0) software input file. In addition to uplift pressure in cracks following forces are considered: (i) weight of the dam and (ii) hydrostatic force at the upstream face of the dam. The values of uplift pressures and model parameters obtained at the level of desired accuracy are finally used to compute the factor of safety of dam against sliding.

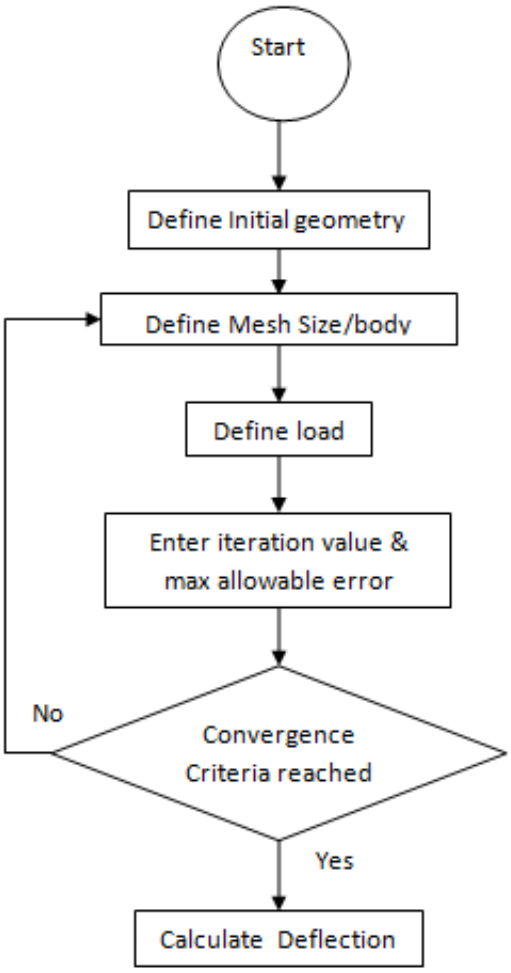

Fig.4.8. Flow chart for dam-crown deflection.

4.5 Summary

Rihand dam is inflicted with multiple cracks caused due to various factors. CMOD rate caused due to creep in FPZ of each cracks are affected by (i) fatigue caused due to reservoir level variations and (ii) interactions of multiple cracks etc. Therefore, after several trials for choosing the CMOD rate generating functions, one that provides the satisfactory result, are chosen. Same criteria have been used to find the number, geometry, and locations of cracks at upstream face of the dam.

Computational procedures essentially consist of three parts: (i) calculation of transient uplift pressure caused due to crack wall motion, (ii) dam-crown deflections under monthly reservoir level variations and (iii) stability analysis of dam in sliding. Transient uplift pressures in the cracks are calculated separately for opening and closing cycle of the crack wall motion. Computed uplift pressures in different cracks at given monthly reservoir level are used with other imposed loads to calculate the dam-crown deflections. Calculated dam-crown deflections are compared with field data until desired accuracy is achieved. The values of uplift pressures and model parameters obtained at the level of desired accuracy are finally used to compute the factor of safety of dam against sliding. A general flow chart for calculating the transient uplift pressure and dam-crown deflection is also presented.